Repeaterless transmission of 40-Gbit/s OTDM signal over long legacy fibre span using unidirectional forward Raman amplification

MOUSAAB M. NAHAS*
Department of Electrical and Electronic Engineering, College of Engineering, University of Jeddah, Jeddah, Saudi Arabia

This paper demonstrates experimental results for 40-Gbit/s OTDM transmission over single in-line fibre span using unidirectional forward Raman amplification. The experiment uses legacy dispersion-managed SMF-DCF configuration where remote EDFAs are used to compensate for the DCF span losses. We successfully show that the transmission performance improves considerably with forward Raman pumping if we apply the appropriate signal wavelength, Raman pump power and remote EDFAs gain. As a result, repeaterless transmission over 206-km SMF is practically achieved using 1545-nm signal wavelength, 1.6-W Raman power and unsaturated Erbium gain into the DCF spans. We believe that such investigation results can be exploited to upgrade network sections that still use legacy fibres without the need for major alteration.

(Received February 13, 2019; accepted December 10, 2019)

Keywords: Fibre-Optics, OTDM, Raman Amplification

1. Introduction

It is well-known that Raman amplification refers to the stimulated Raman scattering (SRS), in which data signal is amplified via nonlinear power transfer from an intense pump signal propagating simultaneously through the fibre [1]. It is also known that the injection of such pump signal into the fibre can be either unidirectional or bidirectional. Obviously, unidirectional pumping involves either forward or backward injection, while bidirectional pumping involves both forward and backward injection simultaneously. In practice, backward Raman is commonly applied due to its better amplification results [2]. In reality, Raman amplifiers have been implemented in long-haul fibre networks since the early part of the 20th century [3]. Unlike repeatered systems, Raman amplification can provide repeaterless transmission with improved noise figure and flattened gain profile.

In fact, plenty of researches have already presented successful repeaterless transmission results using Raman amplification. Many of these experiments used single or multiple 10-Gbit/s wavelength-division multiplexed (WDM) signals [4-7], where many others involved higher bit-rates through optical time-division multiplexing (OTDM), as considered in this paper. However, some of these OTDM projects used all-Raman amplification that is split between the single-mode fibre (SMF) and dispersion compensating fibre (DCF) spans, thus no remote amplification was applied [8]. In other projects, unconventional large effective area fibre (LEAF) was used such that the nonlinear penalty was significantly reduced including the SRS. This in turn required high Raman pump power to enhance the amplification gain [9-11]. Other unconventional fibres were also used including dispersion-shifted fibre (DSF) and non-zero dispersion-shifted fibre (NZ-DSF) [12-13] that are not concerned with in this study. In other project [14], conventional SMF was used but the authors applied bidirectional Raman pumping, which is also not considered in our investigation. Afterwards, some researchers used conventional SMF in all-distributed Raman configuration [15-16], where multiple Raman modules were distributed over short or medium SMF spans. Thus, repeaterless transmission over long span was not demonstrated in such projects. Nevertheless, unidirectional Raman results on long conventional fibres were presented [17] using 2^7-1 data length, since the experiments were too old. In later project, longer data sequence (of 2^{31}-1 length) in 40-Gbit/s transmission over unrepeatered SMF was investigated using backward Raman amplification [18].

This paper aims to investigate the application of forward Raman amplification over long SMF span, using 40-Gbit/s OTDM signal with 2^{31}-1 sequence again. The data signal is transmitted using intensity modulation with direct detection (IM/DD) in return-to-zero (RZ) modulation format. This scheme is chosen to minimize the complexity of the transmitter and receiver designs. It can also encourage upgrading any existing legacy systems without substantial alteration.

2. Experimental setup

The experimental setup for this investigation is shown in Fig. 1. A 10-GHz electrical signal is produced by an RF generator to drive a narrow-pulse laser source and a pulse pattern generator (PPG) simultaneously. The PPG generates a pseudo-random binary sequence (PRBS) with

2^{31}-1 length that is used to modulate the laser signal at a $LiNbO_3$ intensity modulator (IM) [19]. The output of this section is obviously a 10-Gbit/s RZ-IM signal. Since the laser source employed here is capable of generating extremely narrow optical pulses, a Mach-Zehnder optical time-division multiplexing circuit (MZ-OTDM) is then used to increase the bit-rate up to 40 Gbit/s. Fig. 2 shows the MZ-OTDM circuit setup, where the 10-Gbit/s signal, whose pulse time window is 100 ps, is initially split into two equal portions. One of the portions is delayed by 50 ps, and then it couples back with the other undelayed portion. Polarisation controller (PC) is used in one arm just to equalise the polarisation of the two arms. The result of this stage is 20-Gbit/s OTDM signal. By repeating this process again with 25-ps delay, an output signal of 40 Gbit/s is resulted.

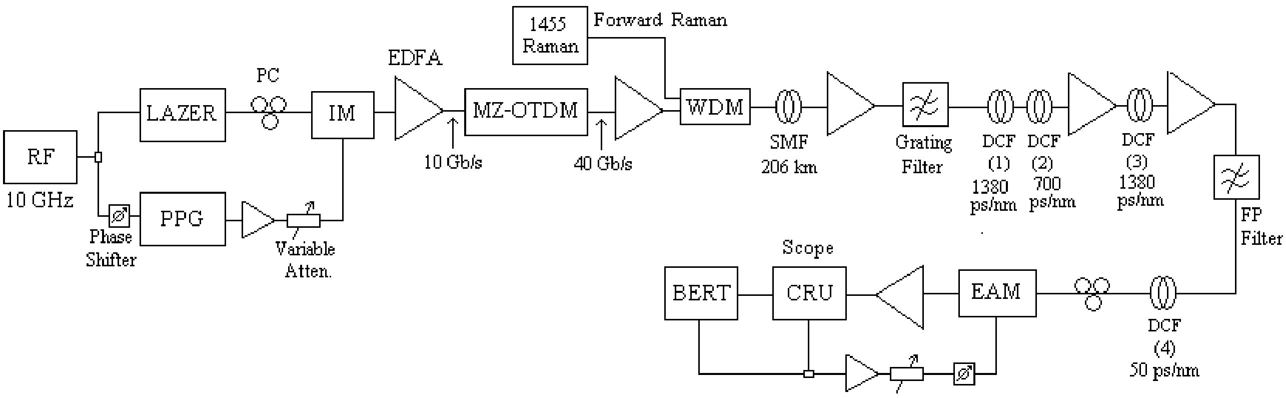

Fig. 1. Experimental setup

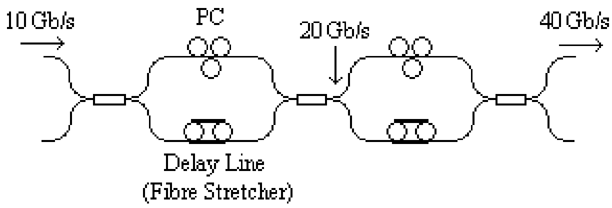

Fig. 2. MZ-OTDM circuit

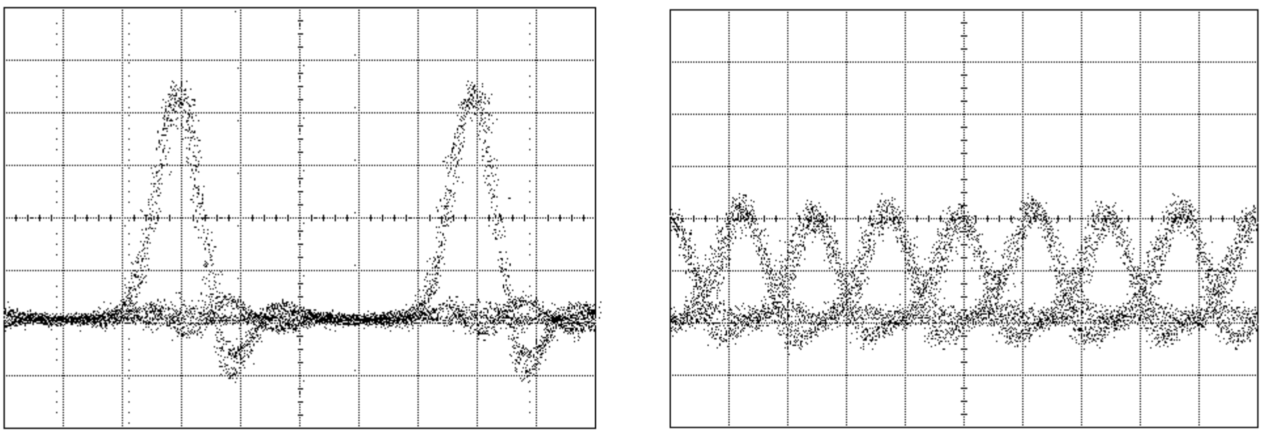

(a) (b)

Fig. 3. (a) MZ-OTDM input 10-Gbit/s signal; (b) MZ-OTDM output 40-Gbit/s signal

In practice, the above delays are not properly sufficient for adequate mixing of bits as they would result in sequential bit repetition within the combined 40-Gbit/s random data. Therefore, additional 100-ps delay (one time widow) is used to avoid such an effect [18]. Fig. 3 (a) shows the input 10-Gbit/s signal to the MZ-OTDM, and (b) shows the output 40-Gbit/s OTDM signal.

The 40-Gbit/s signal is boosted by an Erbium-doped fibre amplifier (EDFA) and then transmitted over a 206-km SMF span. The fibre attenuation coefficient is measured to be ~0.2 dB/km around 1550 nm, while the total dispersion measurement gives ~3510 ps/nm. This amount of dispersion is compensated by the four consecutive DCF sections installed before the receiver. The loss of the SMF span is aimed to be compensated by forward Raman amplification, while the DCF span losses are compensated by the cascaded EDFAs shown in the setup. The DCF attenuation is measured to be ~0.5 dB/km in all spans, and the noise figure of all EDFAs is ~5 dB. Two filters, including Grating and Fabry-Perot (FP) types, are used to eliminate the accumulative ASE noise around the operating wavelength.

At the receiver, a single 10-Gbit/s data signal must be demultiplexed from the 40-Gbit/s OTDM signal for measurements and analysis. Since each pulse occupies a 25-ps window in the 40-Gbit/s bit stream, we need to create a 25-ps switching window every 100 ps to extract a 10-Gbit/s signal. To achieve this, an electro-absorption modulator (EAM) is used to absorb the unwanted three signals and leave only one pulse in the time window. The EAM is initially driven by a 10-GHz electrical clock generated by a clock recovery unit (CRU), and then it is driven through feedback clock recovery. The signal phase can be adjusted using a phase shifter, which enables sliding the switching window in the time domain, giving the ability to choose any pulse among the four OTDM pulses. Finally, the output 10-Gbit/s signal is isolated and pre-amplified for direct detection and measurement.

3. Results and discussion

Firstly, Fig. 4 shows the back-to-back demultiplexed RZ signal acquired from the transmitter-receiver setup illustrated in Fig. 1, using EAM input power of −1 dBm. It is obvious that the receiver is successful in extracting a single 10-Gbit/s signal out of the entire OTDM signal, where the original narrow pluses are cleanly recovered and no errors are counted on the bit-error-rate tester (BERT).

Secondly, by transmitting the OTDM signal over 206 km, it is initially observed that the performance largely depends on the operating wavelength. This is expected in practice due to considerable chirp variation in most laser sources that produce narrow pulses. Therefore, it is essential to identify the optimum wavelength for this system before applying Raman amplification. Fig. 5 shows the signal bit-error-rate (BER) as a function of wavelength using 17-dBm launched power and Erbium amplification only. As a result, the minimum BER is found to be around 1545 nm, thus it is decided to be the operating wavelength for our system. Obviously, the BER is not aimed to be optimised at this point as it is used here just for comparison and wavelength selection purpose. Also, we use high launched power intentionally to introduce nonlinear penalty during the comparison.

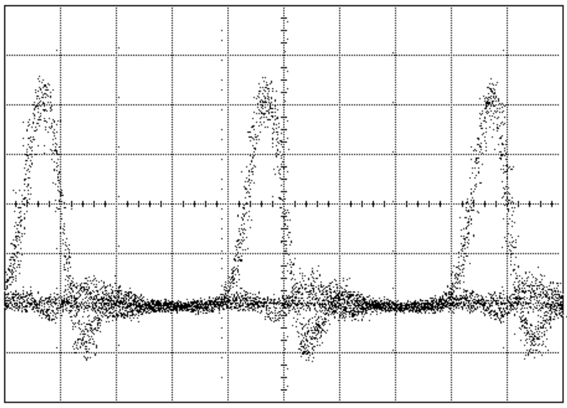

Fig. 4. Back-to-back 10-Gbit/s signal

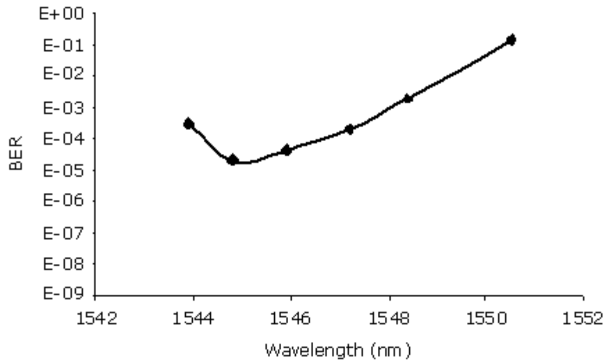

Fig. 5. Signal BER vs operating wavelength

Thirdly, to apply forward Raman amplification, the signal launched power is reduced to 13 dBm to match the saturation power of the existing in-line EDFAs and to minimise the nonlinear penalty in the data signal. Therefore, the Erbium gains are initially set at their maximum level, so that they compensate for the DCF spans attenuation as well as all additional losses due to filters, connectors, splices etc. The total insertion loss of the two in-line filters is measured to be ~10 dB.

By injecting a forward Raman pump signal at 1455 nm into the 206-km SMF, the received signal is significantly impaired and it counts considerable number of errors on the BERT. This can be justified by Fig. 6 that shows the output spectra from the first in-line EDFA, i.e. after the SMF, using different pump power options including ~0.1, 0.9 and 1.6 W. These values are also denoted as 40%, 70% and 100%, respectively, according to the power percentage in the existing Raman module. It is clearly seen that the ASE noise caused by lumped Erbium amplification plays an important role in the overall system performance. In particular, the ASE peak at 1530 nm becomes high at low Raman power, resulting in sever degradation in the total optical signal-to-noise ratio (OSNR). In contrast, the ASE peak moves to greater wavelengths (> 1550 nm) at high Raman power. However, there is an undesired nonlinear interaction between the intense Raman signal and the ASE peak, which in turn corrupts the OTDM pulses. At medium and upper medium Raman power, the gain profile is somewhat flattened but the OSNR is insufficient to yield an acceptable BER. Consequently, the entire noise characteristics depicted in Fig. 6 accumulate in the subsequent EDFAs, causing a serious closure in the received eye diagram, as shown in Fig. 7.

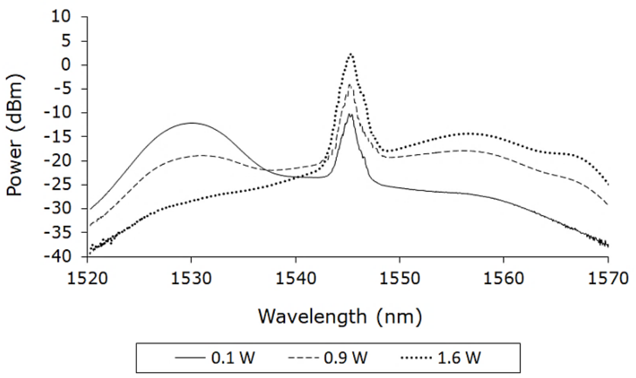

Fig. 6. Gain profile for different Raman power using saturated EDFAs

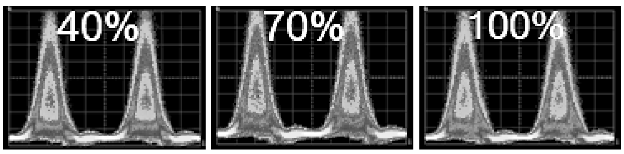

(a) (b) (c)

Fig. 7. Received 10-Gbit/s eye diagram for different Raman power: (a) 0.1 W; (b) 0.9 W; (c) 1.6 W

To solve the above problem, the lumped EDFA gains are empirically reduced such that the accumulated ASE profile is considerably improved and the entire gain spectrum is nearly flattened. As a result, all EDFA gains are reduced by ~2 dB and they no longer operate near saturation. This in turn allows saving some Erbium gain and applying forward Raman amplification comfortably. In effect, the Raman gain compensates for the drop in the Erbium gains, thus the signal average power throughout the whole system is nearly balanced. Therefore, the signal performance is now improved with Raman power rather than degraded as before, where the OSNR is significantly enhanced and the undesired nonlinear interaction due to ASE peak is eliminated. Table 1 shows the received 10-Gbit/s BER against Raman power.

As a result, successful transmission of the intended 40-Gbit/s OTDM signal is achieved where the best result is obtained with Raman power ~1.6 W. The eye diagram of the recovered 10-Gbit/s signal is presented in Fig. 8. We believe that this result is satisfactory for forward Raman amplification, and there is no necessity to afford a higher Raman power module for such system. However, forward error correction (FEC) techniques can rather be applied to reduce the BER for all cases presented in Table 1.

Table 1. Signal BER versus Raman pump power

Raman Power		**BER**
(%)	**(W)**	
40	0.1	$\sim 10^{-4}$
50	0.4	$\sim 10^{-5}$
60	0.6	$\sim 10^{-5}$
70	0.9	$\sim 10^{-6}$
80	1.1	$\sim 10^{-6}$
90	1.4	$\sim 10^{-8}$
100	1.6	$\sim 10^{-9}$

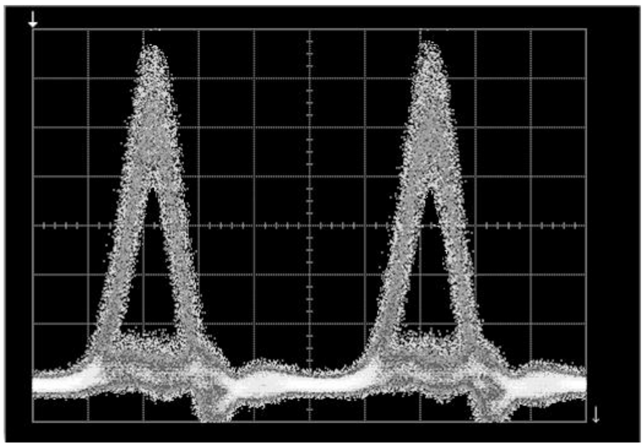

Fig. 8. Received signal obtained by 1.6-W Raman pump and unsaturated Erbium gain

Lastly, the above results can encourage upgrading systems that still use traditional fibre types/configurations, where the study can be extended to simulate ultra-long-haul systems by using a recirculating loop [20-21]. Such large systems are originally composed of multiple fibre spans that are typically << 200 km and are conventionally amplified using in-line EDFA repeaters. Such short spans can be combined to form longer repeaterless spans (of ~200 km, for instance) over which Raman amplification is applied. The main goal for these ultra-long systems would be reducing the required Erbium gain such that the total number of EDFAs is considerably reduced while the overall performance is improved due to Raman amplification.

4. Conclusions

This paper presented repeaterless transmission of 40-Gbit/s OTDM signal over 206 km of conventional SMF span using forward Raman amplification. The experiment used dispersion-managed SMF-DCF configuration, so that Raman amplification was applied to compensate for the SMF loss while remote EDFAs were used to compensate for the DCF losses. The system was optimised with respect to the operating wavelength, Erbium gain profile and Raman pump power. As a result, successful transmission of the intended OTDM signal was achieved using 1545-nm signal wavelength, 1.6-W Raman power and unsaturated gains in the lumped EDFAs.

Acknowledgments

The author thanks Aston Photonics Group for their assistance in some parts of the research.

References

[1] R. W. Boyd, Nonlinear Optics, Academic Press, (2013).
[2] G. P. Agrawal, Nonlinear Fibre Optics, Academic Press, (2019).
[3] M. Islam, IEEE Journal of Selected Topics In Quantum Electronics **8**, 548 (2002).
[4] Z. Xu, J. Seoane, A. Siahlo, L. Oxenlewe, A. Clausen, P. Jeppesen, Conference on Lasers and Electro-Optics (CLEO)**,** 2 (2004).
[5] M. Haris, J. Yu, G. K. Chang, IEEE Lasers and Electro-Optics Society (LEOS), WE1, 479 (2005).
[6] H. Maeda, G. Funatsu, A. Naka, Electronics Letters **41**, 34 (2005).
[7] R. Jee, S. Chandra, International Conference on Advances in Computing, Communications and Informatics (ICACCI), 172 (2015).
[8] Z. Huang, A. Gray, Y. Lee, I. Khrushchev, I. Bennion, Conference on Lasers and Electro-Optics (CLEO), 531 (2003).
[9] G. Charlet, M. Salsi, P. Tran, M. Bertolini, H. Mardoyan, J. Renaudier, O. Bertran-Pardo, S. Bigo, Optical Fibre Communication Conference, PDPB6 (2009).
[10] D. Chang, W. Pelouch, P. Perrier, H. Fevrier, S. Ten, C. Towery, S. Makovejs, Optics Express **22**, 31057 (2014).
[11] H. Bissessur, C. Bastide, S. Dubost, S. Etienne, Optical Fibre Communications Conference and Exhibition (OFC), 1 (2015).
[12] H. Masuda, H. Kawakami, S. Kuwahara, A. Hirano, K. Sato, Y. Miyamoto, Electronics Letters **39**, 1668 (2003).
[13] D. Rafique, T. Rahman, A. Napoli, R. Palmer, J. Slovak, E. Man, S. Fedderwitz, M. Kuschnerov, U. Feiste, B. Spinnler, B. Sommerkorn-Krombholz, M. Bohn, IEEE Photonics Technology Letters **27**, 1911 (2015).
[14] P. Rosa, N. Murray, R. Bhamber, J. Ania-Castañón, P. Harper, European Conference on Optical Communications (ECOC), 1 (2012).
[15] D. Chang, S. Burtsev, W. Pelouch, E. Zak, H. Pedro, W. Szeto, H. Fevrier, T. Xia, G. Wellbrock, Optical Fibre Communications Conference and Exhibition (OFC), 1 (2014).
[16] S. Burtsev, H. Perdo, D. Chang, W. Pelouch, H. Fevrier, S. Ten, S. Makovejs, C. Towery, Optical Fibre Communications Conference and Exhibition (OFC), 1 (2015).
[17] M. Gunkel, F. Kiippers, J. Berger, U. Feiste, R. Ludwig, C. Schubert, C. Schmidt, H. Weber, Electronics Letters **37**, 646 (2001).
[18] M. Nahas, Journal of Electrical and Electronic Engineering **3**, 127 (2015).
[19] M. Wahid, M. Nahas, R. Ibbotson, K. Blow, Optics Communications **332**, 55 (2014).
[20] M. Nahas, K. Blow, IET Communications **8**, 800 (2014).
[21] M. Nahas, Optoelectron. Adv. Mat. **12**(9-10), 536 (2018).

*Corresponding author: mnahas1@uj.edu.sa